The Cryosphere, 6, 479–491, 2012
www.the-cryosphere.net/6/479/2012/
doi:10.5194/tc-6-479-2012

The Cryosphere

Albedo of the ice covered Weddell and Bellingshausen Seas

A. I. Weiss, J. C. King, T. A. Lachlan-Cope, and R. S. Ladkin

British Antarctic Survey, National Environment Research Council, High Cross, Madingley Road, Cambridge, CB3 0ET, UK

Correspondence to: A. I. Weiss (aiw@bas.ac.uk)

Received: 13 October 2011 – Published in The Cryosphere Discuss.: 30 November 2011
Revised: 15 March 2012 – Accepted: 26 March 2012 – Published: 11 April 2012

Abstract. This study investigates the surface albedo of the sea ice areas adjacent to the Antarctic Peninsula during the austral summer. Aircraft measurements of the surface albedo, which were conducted in the sea ice areas of the Weddell and Bellingshausen Seas show significant differences between these two regions. The averaged surface albedo varied between 0.13 and 0.81. The ice cover of the Bellingshausen Sea consisted mainly of first year ice and the sea surface showed an averaged sea ice albedo of $\overline{\alpha_i} = 0.64 \pm 0.2$ ($\pm$standard deviation). The mean sea ice albedo of the pack ice area in the western Weddell Sea was $\overline{\alpha_i} = 0.75 \pm 0.05$. In the southern Weddell Sea, where new, young sea ice prevailed, a mean albedo value of $\overline{\alpha_i} = 0.38 \pm 0.08$ was observed. Relatively warm open water and thin, newly formed ice had the lowest albedo values, whereas relatively cold and snow covered pack ice had the highest albedo values. All sea ice areas consisted of a mixture of a large range of different sea ice types. An investigation of commonly used parameterizations of albedo as a function of surface temperature in the Weddell and Bellingshausen Sea ice areas showed that the albedo parameterizations do not work well for areas with new, young ice.

1 Introduction

The albedo α is defined as the ratio of short wave outgoing Sw_{up} to short wave incoming radiation Sw_{down}. In polar regions sea ice exerts a strong control on the sea surface albedo. Trends in the satellite-derived Antarctic sea ice concentrations (1979–2002) show a clear decrease in the Bellingshausen and western Weddell Seas by about 4–10 % per decade (Liu et al., 2004). This may have been caused by a temperature change, as since the 1950s a major warming trend has been observed in annual mean temperature on the western side of the Antarctic Peninsula of about 0.56 °C per decade. The largest statistically significant temperature increase on the eastern side of the Antarctic Peninsula occurred during summer (Turner et al., 2006). In order to investigate effects of such a sea ice decrease in the Antarctic on the climate system, climate model studies have to be performed, which require accurate specification or parameterization of the albedo. However, the Antarctic is a region where there is a large spread in the predictions of future climate between different models (Bracegirdle et al., 2008). One reason for this might be that the Antarctic sea ice zone remains one of the least known regions on Earth and only few direct observations of the albedo in the Antarctic sea ice zone exist so far (e.g. Predoehl and Spano, 1965; Allison et al., 1993; Pirazzini, 2007; Zhou et al., 2007; Vihma et al., 2009; Brandt et al., 2005).

To deepen our understanding of the albedo of Antarctic sea ice areas, we have analyzed aircraft-based field measurements conducted by the British Antarctic Survey in the austral summers of 2006/2007 and 2007/2008. Our study has three main goals. First, we aim to determine regional differences in the sea surface albedo between the Bellingshausen Sea and the western Weddell Sea. We then attempt to explain these differences in terms of sea ice parameters that influence the sea surface albedo, such as the average percentage of prevailing sea ice type, sea ice concentration, snow cover and by the surface temperature. In order to describe the surface albedo in the sea ice area representative of the non-homogenous sea surface, area-averaged albedo values of the sea surface need to be known. Area-averaged albedo values of the non-homogenous sea ice area can be a composite of albedo values of open water in leads and polynyas, bare ice or various kinds of snow covered ice of different age. Therefore, the second goal of this study is to determine typical area-averaged sea ice albedo values, which are representative

of sea ice areas adjacent to the Antarctic Peninsula in summer. Most climate and numerical weather prediction models cannot take into account all of the factors that influence the albedo in the sea ice area. The main reason for this is that not all the necessary information is available in a model as input parameters for a complex albedo parameterization. In fact, very often the albedo parameterizations in numerical models are relatively simple and assume a constant value for a model grid cell or parameterize the sea ice albedo solely with the surface temperature. The surface temperature is not a good physical predictor for the albedo of the ice covered sea, but the temperature is an input variable, which is available in most models. These parameterizations use the fact that the surface temperature acts as a proxy for physical parameters, which influence the radiative properties of the ice covered sea surface, such as thickness of the ice, snow cover, snow grain size and amount of brine in the sea ice. Up to now, sea ice albedo parameterization schemes were largely determined and validated with data sets that were collected in the Arctic (e.g. Curry et al., 2001) and little is known about how well those parameterization schemes perform for Antarctic sea ice areas. Therefore, the third goal of this study is to address the relation between temperature and albedo in Antarctic sea ice zones. We investigate whether commonly-used albedo parameterizations, which use the temperature as the sole input forcing parameter, are appropriate to describe the albedo of the sea ice areas in the western Weddell Sea and the north-eastern Bellingshausen Sea in summer.

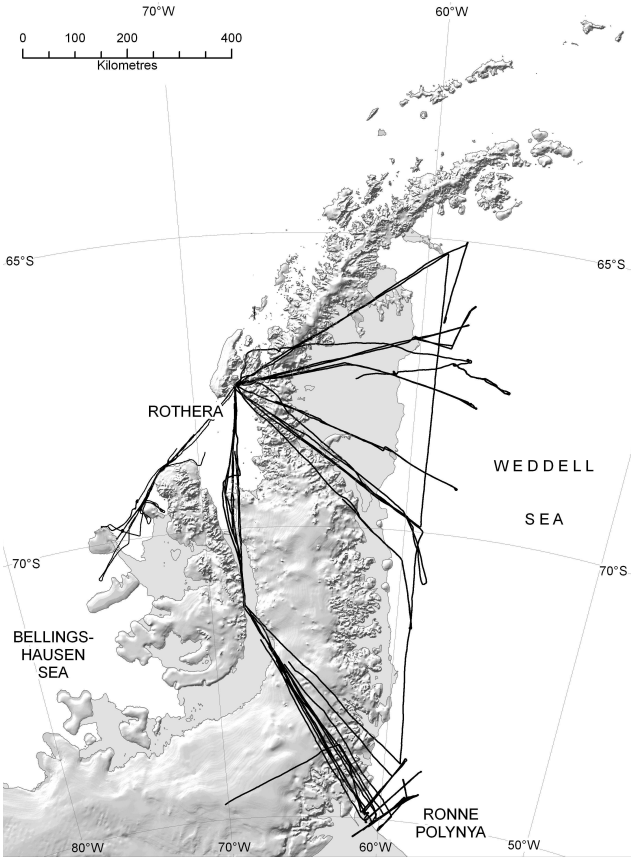

Fig. 1. Map of Antarctic Peninsula with flight tracks (black lines) flown during the aircraft field campaigns 2007 and 2008, which form the basis of this study.

2 Methods

2.1 Observational area

Airborne observations of sea surface albedo in the Antarctic were carried out during two austral summer measurement campaigns. The first campaign took place during February and March 2007 and the second during January and February 2008. Measurements were made using an instrumented DHC6 Twin Otter aircraft operated by the British Antarctic Survey. All flights started from Rothera Research Station on Adelaide Island (67.6° S, 68.1° W). During these two campaigns the sea surface albedo was measured in the area of the western Weddell Sea (around 65° S–75° S, 55° W–61° W) and in the north-eastern Bellingshausen Sea (68.6 ° S–69.9 ° S, 70.8° W–75.6° W). Figure 1 shows a map of the Antarctic Peninsula with the flight tracks (black lines) of the 2007 and 2008 campaigns, which form the basis of this study. Most albedo measurements were taken under clear sky to partly cloudy conditions. During some flights the cloud conditions varied temporally and spatially. The cloud conditions during the Bellingshausen Sea flights can be described as mainly clear sky with some cirrus clouds and partly cloudy with cirrus clouds. During the Weddell Sea flights, we observed mainly clear sky and partly cloudy conditions with cirrus clouds, but in some other areas we observed cumulus convection over leads and polynyas, overcast conditions with stratus clouds and sea smoke over thin ice.

The albedo measurements, which are presented in this study, were mainly conducted over a compact ice covered sea surface. The amount of sea ice is determined by the sea ice mass balance, i.e. by the amount of sea ice, which is produced or melted. In the Antarctic there is a strong interannual and spatial variation of the sea ice mass balance. The melt season is driven mainly by the solar radiation and the onset of melt occurs in the austral spring season. The main factors that influence the sea ice mass balance are the air and sea surface temperature, heat fluxes at the top, bottom and boundaries of the sea ice, sea ice brine volume, snow cover and thickness, the sea ice albedo, the movement of ice by wind and ocean current and the salinity of the sea (because it influences the freezing point of sea water). The salinity varies between the Weddell and the Bellingshausen Seas. An overview of oceanic parameters in the Weddell Sea can be found by Nicholls et al. (2001, 2008). The typical regional surface salinity in the southern part of the western Weddell Sea is around 33.5 to 34.1, which results in a freezing

point of $T_s = -1.84\,°C$ to $-1.89\,°C$. Oceanographic measurements in the Bellingshausen Sea (Jenkins and Jacobs, 2008) showed that the surface salinity in this sea ice area varies around 32.7 to 33.5, which leads to a freezing point between $T_s = -1.79\,°C$ and $-1.84\,°C$.

2.2 Aircraft instrumentation

The aircraft was instrumented with upward- and downward-facing pyranometers (Eppley, PSP) to measure short wave radiation, and upward- and downward facing pyrgeometers (Eppley, PIR) to measure long wave radiation. The radiometers have a 2π viewing angle, i.e. a hemispheric view. However, the irradiance, which is detected by the upward directed pyranometer, is controlled by the cosine of the solar zenith angle. The cosine response of the PSP pyranomenters is 1 % for 0–70° from zenith (which can be assumed for the data of this study) and 3 % for 70–80° from zenith. The broadband albedo (in this study simply called albedo) of the surface was determined from the ratio of the upward- and downward-facing pyranometer data. The pyranometers provide an albedo value in the wavelength range of 0.285 µm to 2.8 µm. The logging frequency of all radiometers was 10 Hz. Raw data from the upward-facing pyranometer was corrected for aircraft attitude variations according to Bannehr and Glover (1991). For the determination of the aircraft position and attitude, we used a JAVAD AT4 four-antenna GPS system. This GPS system gives all three components of aircraft position, attitude and velocity at a rate of 20 Hz. The resolution of the pyranometers is about $0.5\,W\,m^{-2}$ and they measure with an estimated absolute accuracy of 3 %. The downward-facing radiation sensors were mounted on the underside of the aircraft together with a downward-looking video camera and a Heimann KT 19.82 infrared thermometer (IRT). The lens of the IRT provides a field of view of the sea surface of 4.42 m (diameter) at a flight height of 100 m. The resolution of the IRT lies in the range of 0.1 °C. The IRT sensor on the aircraft enabled the recording of the sea surface temperature along the flight tracks. In order to minimize errors due to non-optimal working temperatures of the IRT on the aircraft, the sensor was insulated. The IRT detector has a spectral sensitivity in the range of 8 µm to 14 µm, i.e. the sensitivity range lies in a water vapor window of the atmosphere. In this spectral range the transmission of the atmosphere for infrared wavelengths is relatively high. To reduce the remaining error due to absorption and emission by atmospheric gases, we conducted the observations at relatively low flight levels at heights around 20 m to 80 m. We account for remaining emission and absorption effects by the intervening atmosphere between aircraft and surface by using a constant correction factor, as described by Burns et al. (2000). We estimate the accuracy of the IRT in the range of 0.5 °C. A detailed description of the instrumental setup on the Twin Otter aircraft is given by King et al. (2008) and Weiss et al. (2011).

2.3 Determination of sea ice concentration

To obtain information about the sea ice concentration C_{ice}, we analyzed measurements from the IRT, the pyranometers and the video camera. The sea ice concentration was calculated by discriminating between ice and open water, using thresholds for surface temperature (freezing point) and albedo. To determine the threshold for temperature, i.e. the freezing point, we assessed the typical salinity of the surface sea water for the three main sea ice areas: we assumed a mean surface sea water salinity of 34.0 for the Weddell Sea pack ice region and estimated the freezing point of the sea water to be $T_f = -1.87\,°C$. For the southern part of the western Weddell Sea, in the Ronne Polynya region, we assumed a mean salinity of 34.5 and estimated the freezing point to be $T_f = -1.89\,°C$ and for the north-eastern part of the Bellingshausen Sea, we assumed a mean value of the salinity of 33.1 and of the sea water freezing point of $T_f = -1.81\,°C$. The freezing points were used to distinguish between ice and open water in combination with an albedo value threshold of $\alpha_w < 0.07$ for open water and of $\alpha_i \geq 0.07$ for the ice covered sea surface. With this algorithm we determined, from the high resolution 10 Hz data, remotely the sea ice concentration of each flight. This method gives only an approximation of the sea ice concentration, because we use a mean salinity value and moreover, the field of views of the pyranometers and the IRT are different as described in Sect. 2.2. We quantified the error of the sea ice concentration data of this study due to the unknown precise sea ice salinity. This error is small, in the range of per mill or less for our data. However, due to the fact that the field of view of the IRT is smaller than that of the pyranometers, an over- or underestimation of the irradiance for the sea ice area that the IRT is detecting can result. This would be the case, in particular, for sea ice areas that show a strong heterogeneous sea surface due to a mixture of water or thin dark ice and solid white sea ice. However, most of our measurements presented in this study were conducted at low surface temperatures and over relatively compact sea ice with small water fraction. To improve our concentration estimates, we additionally used video footage, which often enables one to discriminate visually between thin dark ice and open water patches.

3 Observations and results

3.1 Sea ice characteristics

The ice covered sea surface in the north-eastern Bellingshausen Sea in February 2007 was comprised of a mixture of different first year sea ice types such as thin white ice, medium and thick first year ice and snow covered first year ice. By contrast, during the 2008 observing campaign, this region was almost ice free. The floe size of the first year ice, which we observed in February 2007, ranged typically from

less than 20 m across to medium floes with diameters ranging from 100 m to 500 m. Between the floes we observed slush and frazil ice and/or nilas and icebergs. Corresponding to this wide range of surface types, the sea surface in the north-eastern Bellingshausen Sea showed a large range of albedo and surface temperature values in 2007. A typical example of the sea ice conditions in the north-eastern Bellingshausen Sea is given in the left panel of Fig. 2. The picture shows the ice conditions that we observed on 26 February 2007. During that day, lowest albedo values were around $\alpha_{\min} = 0.06$ and correspond to surface temperatures of open water. The highest albedo values reach more than $\alpha_{\max} \geq 0.8$ and correspond to surface temperatures in the range of about $-9.0\,^{\circ}\mathrm{C} < T_{\mathrm{s}} \leq -6.0\,^{\circ}\mathrm{C}$. These high albedo values at low surface temperatures are characteristic of snow covered sea ice (e.g. Brandt et al., 2005).

In the western Weddell Sea, we deduced from visual observations that the fast ice adjacent to the Larsen Ice Shelf can be characterized mainly as snow covered multi-year pack ice. The main reason for sea ice remaining over more than one season in the western Weddell Sea is the prevailing ocean current. In the central Weddell Sea the clockwise-directed Weddell Gyre traps the sea ice along the east coast of the Antarctic Peninsula. The Weddell Gyre transports the sea ice relatively slowly. During both campaigns, in 2007 and 2008, we observed that the pack ice in the western Weddell Sea seldom formed a closed cover, but polynyas and leads were present. Leads and polynyas persist as open water, but when temperatures drop below the freezing point, grease ice, nilas and grey ice form rapidly on their surface. The middle panel of Fig. 2 displays a typical picture of the western Weddell Sea pack ice area (16 February 2007). During this example the lowest albedo values of $\alpha_{\min} = 0.07$ were observed and they corresponded to sea surface temperatures of $T_{\mathrm{s}} = -1.9\,^{\circ}\mathrm{C}$ near the freezing point of sea water. Visually, we observed hardly any patches of open water, but very thin, dark ice during this flight. The largest albedo values of more than $\alpha_{\max} \geq 0.8$ were observed at surface temperatures around $T_{\mathrm{s}} = -8.0\,^{\circ}\mathrm{C}$, which we visually allocate to snow covered pack ice. The reason why snow covered sea ice has a higher albedo than snow free ice is due to the fact that snow consists of a large number of grains, which increase the scattering of the incoming radiation. Wiscombe and Warren (1980) showed with a radiative transport model that the albedo decreases as the grain size increases. This is due to the fact that larger grains are both more absorptive and more forward scattering.

In the southern part of the western Weddell Sea a polynya persists off the front of the Ronne Ice Shelf, known as the Ronne Polynya. In the Weddell Sea it has been estimated that the area coverage of the polynyas and leads is about 5 % (Schnack-Schiel, 1987). The Ronne Polynya is the result of the ocean current and of the prevailing wind in this area. The wind direction is mostly southerly to south-easterly, resulting from cold air draining from the continent. The ocean current follows the barrier of the Ronne Ice Shelf westwards. The size of the Ronne Polynya varied between our flight missions, because new, young and grey ice formed rapidly on open water in this area when the air temperatures dropped below the freezing point, in particular during cold air outflows from the Ronne Ice Shelf. A picture of the new, young and grey ice covered polynya area, taken on 25 February 2007, is shown in the right panel of Fig. 2. In this example the surface albedo ranged from $\alpha_{\min} = 0.07$ up to $\alpha_{\max} = 0.9$ within a surface temperature range of $T_{\mathrm{s}} = -1.5\,^{\circ}\mathrm{C}$ to $T_{\mathrm{s}} = -9.7\,^{\circ}\mathrm{C}$. Close to the Ronne Ice Shelf, we measured higher surface temperatures and lower albedo values. 50–100 km away from the Ronne Ice Shelf, the prevailing sea ice became considerably thicker and snow covered, showing lower surface temperatures and the surface albedo increased in this area up to more than $\alpha \geq 0.8$. This is in agreement with ship measurements of the albedo of Brandt et al. (2005).

Based on our observations of the sea surface conditions, for this study we classify sea ice areas adjacent to the Antarctic Peninsula into three main categories: we defined, as the first main sea ice area, the north-eastern Bellingshausen Sea where new, young and first year sea ice prevails; our second main sea ice area is the western Weddell Sea area, where multi-year pack ice eastward of, and adjacent to, the Larsen Ice Shelf persists; our third area is defined as the southern part of the western Weddell Sea, adjacent to the Ronne Ice Shelf, which has mainly a new, young first year sea ice cover in the Ronne Polynya area. The observed sea ice conditions in the three areas are representative of the recent decade in summer. An analysis of 28 yr of Antarctic sea ice data derived from satellite passive microwave radiometers (Cavalieri and Parkinson, 2008) showed that in the western Weddell Sea, the mean sea ice concentration in February is between 90–100 % and that the sea ice concentration in the northern part of the Bellingshausen Sea is much lower and can vary from <12 % up to 100 %. In the last ten years, multi-year pack ice was mainly observed in the western Weddell Sea and in the southern part of the Bellingshausen/Amundsen Sea, and first year ice in the northern part of the Bellingshausen Sea in February. In the southern part of the western Weddell Sea, the Ronne Polynya habitually forms off the Ronne Ice Shelf (Renfew et al., 2002). Zwally et al. (2002) discussed the Antarctic sea ice variability. The decadal-scale sea ice change has been small, although the sea ice cover varied from year to year. They found a positive sea ice extent trend in the Weddell Sea (1.4 ± 0.9 %) and a negative trend in the Bellingshausen/Amundsen Sea (-9.7 ± 1.5 %) for the 20 yr period 1979–1998 (Zwally et al., 2002).

3.2 Mean albedo

In order to define characteristic surface values for these three main sea ice areas, we determined, on the basis of the high resolution data for each flight mission, the averaged water $\overline{\alpha_{\mathrm{w}}}$ and sea ice albedo $\overline{\alpha_{\mathrm{i}}}$ (albedo averaged over ice covered

Fig. 2. Pictures of typical sea ice conditions during the field campaign in the north-eastern Bellingshausen Sea (left panel, 26 February 2007), the western Weddell Sea pack ice area (middle panel, 16 February 2007), and the south-western Weddell Sea Ronne Polynya area (right panel, 25 February 2007).

areas only), and their corresponding temperatures $\overline{T_w}$ and $\overline{T_i}$, respectively. They are listed in Table 1. Four flights over the north-eastern Bellingshausen Sea ice area, eleven flights over the western Weddell Sea pack ice area and five flights over first year sea ice in the southern part of the western Weddell Sea form the basis of this study. The sea ice concentration in the Weddell Sea was always high during our observations, i.e. $C_{ice} \geq 95\,\%$. In the north-eastern Bellingshausen Sea, the sea ice concentrations showed lower values with $C_{ice} \geq 73\,\%$. The mean sea ice albedo, which we observed in the Bellingshausen Sea, averaged over an entire flight, ranged from $\overline{\alpha_i} = 0.25$ up to $\overline{\alpha_i} = 0.69$. In the Weddell Sea pack ice areas, we observed higher mean area-averaged sea ice albedo values, ranging from $\overline{\alpha_i} = 0.66$ up to $\overline{\alpha_i} = 0.82$. In contrast to this, we observed the smallest mean sea ice albedo values in the southern part of the western Weddell Sea, where the mean area-averaged albedo ranged from $\overline{\alpha_i} = 0.24$ to $\overline{\alpha_i} = 0.42$. We investigated whether the mean albedo and mean sea surface temperature $\overline{T_s}$ (water and sea ice) are a function of mean sea ice concentration. The mean sea surface albedo and temperature show no clear dependence on mean sea ice concentration in any of the three sea ice areas in our data set. This can be explained by the fact that our observations were collected over very compact sea ice cover. Other studies showed that, with substantial increase of water fraction, the mean sea surface albedo decreases (Brandt et al., 2005). They showed, on the basis of satellite data, that if the ice is pushed northward by the winds and currents, so that there is a substantial fraction of open water on the sea surface, the main determinant of area-averaged albedo becomes the ice concentration.

Figure 3 displays the percentage of sea surface within a given albedo bin ($\Delta\alpha = 0.1$) in the north-eastern Bellingshausen Sea, the western Weddell Sea and south-western Weddell Sea. The distributions show that in all three sea ice areas, we observed a wide range of albedo values, suggesting that all three areas contain a mixture of different sea ice types or mixture of sea ice of different age, snow cover and thickness. In the north-eastern Bellingshausen Sea, we observed that over 30 % of the sea surface had an albedo value less than 0.1, i.e. over 30 % of the surface was sea ice free

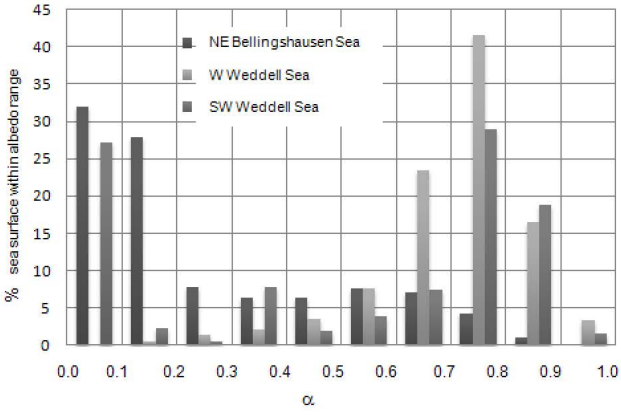

Fig. 3. Percentage of sea surface within a given albedo bin ($\Delta\alpha = 0.1$) in the north-eastern Bellingshausen Sea, the western Weddell Sea and south-western Weddell Sea ice areas.

or covered with newly formed sea ice and dark nilas. In the south-western Weddell Sea polynya region, we observed a similar high percentage of small albedo values below 0.1 (approx. 27 %), which indicates water or dark new ice. The Weddell Sea pack ice region showed, in contrast, less than 1 % of the surface with an albedo less than 0.1, indicative of open water or thin dark ice. In the pack ice area, we observed that more than 80 % of the surface showed albedo values larger than 0.6, which is a typical value for thick, snow covered sea ice.

4 Discussion

4.1 The use of mean albedo in numerical model studies

The knowledge of the mean area-averaged surface albedo can be used to improve numerical model simulations of these areas. Large-scale general circulation models often use a very simple albedo parameterization, which assumes a characteristic surface albedo value within the model grid box. Some models determine the ice cover within each model grid box

Table 1. Date and length of flight missions in the Weddell and Bellingshausen Seas and mean values (as median) of ice concentration C_{ice}, sea ice temperature $\overline{T_{\mathrm{i}}}$, water temperature $\overline{T_{\mathrm{w}}}$, sea ice albedo $\overline{\alpha_{\mathrm{i}}}$, and sea water albedo $\overline{\alpha_{\mathrm{w}}}$, for each flight mission with their standard deviations σ.

Date	Flight length [km]	Sea ice only			Water only	
		C_{ice} [%]	$\overline{T_{\mathrm{i}}} \pm \sigma_T$ [°C]	$\overline{\alpha_{\mathrm{i}}} \pm \sigma_\alpha$	$\overline{T_{\mathrm{w}}} \pm \sigma_T$ [°C]	$\overline{\alpha_{\mathrm{w}}} \pm \sigma_\alpha$
NE Bellingshausen Sea (first year ice)						
13 February 2007	396	91	-0.6 ± 0.4	0.65 ± 0.14	-1.1 ± 0.4	0.06 ± 0.01
21 February 2007	176	88	-3.3 ± 0.6	0.69 ± 0.09	0.9 ± 0.2	0.07 ± 0.01
21 February 2007	171	100	-2.5 ± 0.8	0.63 ± 0.09	No open water	No open water
26 February 2007	634	73	-2.9 ± 2.4	0.25 ± 0.2	-0.9 ± 0.6	0.07 ± 0.05
W Weddell Sea (pack ice)						
15 February 2007	365	100	-8.9 ± 1.4	0.80 ± 0.05	No open water	No open water
16 February 2007	327	100	-8.1 ± 2.1	0.75 ± 0.16	No open water	No open water
16 February 2007	212	100	-6.9 ± 1.5	0.76 ± 0.16	Less than 1 % open water	Less then 1 % open water
1 March 2007	387	100	-12.4 ± 2.7	0.82 ± 0.19	Less than 1 % open water	Less than 1 % open water
29 January 2008	257	99	-1.9 ± 0.6	0.68 ± 0.09	-1.1 ± 0.3	0.1 ± 0.0
2 February 2008	459	100	-0.9 ± 0.3	0.69 ± 0.12	Less than 1 % open water	Less than 1 % open water
9 February 2008	563	100	-4.6 ± 0.1	0.79 ± 0.02	Less than 1 % open water	Less than 1 % open water
10 February 2008	538	100	-2.6 ± 0.1	0.75 ± 0.01	Less than 1 % open water	Less than 1 % open water
18 February 2008	181	95	-1.5 ± 0.5	0.66 ± 0.12	-1.2 ± 0.2	0.06 ± 0.01
21 February 2008	277	100	-5.7 ± 1.0	0.74 ± 0.11	No open water	No open water
21 February 2008	312	100	-7.7 ± 1.8	0.73 ± 0.18	No open water	No open water
SW Weddell Sea (new, young sea ice)						
25 February 2007	164	100	-6.6 ± 2.0	0.38 ± 0.29	Less than 1 % open water	Less than 1 % open water
27 February 2007	265	100	-12.3 ± 2.89	0.41 ± 0.12	No open water	No open water
28 February 2007	85	100	-10.7 ± 2.7	0.42 ± 0.10	No open water	No open water
5 February 2008	350	99	-5.8 ± 2.8	0.24 ± 0.29	-1.8 ± 0.1	0.06 ± 0.01
6 Februay 2008	104	100	-3.6 ± 3.4	0.29 ± 0.27	Less than 1 % open water	Less than 1 % open water

and two characteristic albedo values are used, one for the prevailing sea ice type and the second one for open water. With a weighting function the mean albedo in the grid box is determined. There are also models, which assume one albedo value for a model grid box, e.g. a value that is a mean of all albedo values within the grid box. Such a relatively simple albedo parameterization approach is found, for example, in the large-scale sea ice model of Parkinson and Washington (1979), in the atmospherically forced sea ice model of Hibler and Bryan (1987), and the thermodynamic sea ice model of Ross and Walsh (1987), among others. Some models assume a characteristic albedo value for a certain sea ice type. This approach is used, e.g. in the sea ice model of Mellor and Kantha (1989). Lists of typical albedo values of certain sea ice types in Antarctica are given, e.g. by Brandt et al. (2005) and Allison et al. (1993). In some models the sea surface albedo is not parameterized but is a prognostic variable, e.g. in the Goddard Institute for Space Studies (GISS) climate model as described by Hansen et al. (1983), in which the albedo is determined from the albedo value of the previous month. Whether assuming an albedo value or using a prognostic albedo value, both approaches for describing the sea surface albedo have in common that one mean albedo value is used within a grid box. In Table 2 we determined, for the three defined main sea ice areas adjacent to the Antarctic Peninsula from the data listed in Table 1, mean albedo values. We calculated mean albedo values for ice covered surface only and the mean albedo for the open water fraction. The corresponding mean percentage of sea ice cover is also listed in Table 2. Comparing the averaged albedo values for the sea surface consisting of a mixture of water and sea ice to the averaged albedo of the mixture of sea ice without water fraction, the values are almost identical as the sea ice concentration in all three sea ice areas was so high. We observed the largest mean sea ice albedo value of $\overline{\alpha_{\mathrm{i}}} = 0.75$ in the western Weddell Sea pack ice area and the smallest mean albedo value of $\overline{\alpha_{\mathrm{i}}} = 0.38$ south of the pack ice area in the polynya region of the Weddell Sea, where young, new sea ice prevailed. In the north-eastern Bellingshausen Sea, we determined a characteristic mean sea ice albedo of $\overline{\alpha_{\mathrm{i}}} = 0.64$ from our data set.

Table 2. Averaged sea ice albedo of data listed in Table 1 for the north-eastern Bellingshausen Sea, western Weddell Sea and south-western Weddell Sea with average percentage of sea ice cover.

	NE Bellingshausen Sea first year sea ice area	W Weddell Sea pack ice area	SW Weddell Sea new or young sea ice area
Average percentage of sea ice cover	89.2 %	99.9 %	99.9 %
$\overline{\alpha_i} \pm \sigma_\alpha$ (mix of sea ice without open water)	0.64 ± 0.20	0.75 ± 0.05	0.38 ± 0.08
$\overline{T_i} \pm \sigma_{T_i}$ (mix of sea ice without open water)	$-2.7 \pm 1.2\,^\circ$C	$-5.7 \pm 3.6\,^\circ$C	$-6.6 \pm 3.6\,^\circ$C

4.2 Relation between albedo and temperature

In order to investigate the relation between albedo and temperature, we determined a mean albedo value for surface temperature bins of $\Delta T_s = 1\,^\circ$C for each flight. We averaged the binned albedo for all flights within each of the three sea ice areas. The averaged relations for each sea ice area are shown in the upper panels of Fig. 4 for temperatures below the freezing point. All three upper panels in Fig. 4 indicate that the sea ice albedo shows a tendency to increase with a decrease in surface temperature. The only exception was observed in the data of the north-western Bellingshausen Sea, where the highest albedo value was not observed at the lowest surface temperature. The upper panels of Fig. 4 also show that a certain albedo value can occur at various temperatures and that the mean values have, in general, large standard deviations. In the lower panels of Fig. 4, we display the number of data points that were available within each temperature bin. This gives an indication of the mixture of different sea surface temperatures that we observed in the three sea ice areas adjacent to the Antarctic Peninsula. In the north-eastern Bellingshausen Sea, the first year ice shows temperatures between the freezing point and about $T_i = -6\,^\circ$C, but most observations in the Bellingshausen Sea showed surface temperatures around $T_i = -3\,^\circ$C. In the Weddell Sea ice areas, a much larger surface temperature range was observed, ranging from the freezing point to temperatures $T_i \leq -14\,^\circ$C. The large standard deviations indicate that the temperature is not directly linked to the albedo. The surface temperature is acting as a proxy for some of the physical factors, which influences the albedo of the ice covered sea, but there are also factors which depend not directly on the temperature, such as changing cloud cover. Previous experimental and theoretical model studies investigated how factors like solar zenith angle and cloud cover (e.g. Vashisth, 2005; Grenfell and Perovich, 1984), wavelength (e.g. Grenfell et al., 1994), salinity (Perovich and Grenfell, 1981) and snow cover (e.g. Brandt et al., 2005), among other factors influence the radiative properties of sea ice. Vashisth (2005) showed that clouds have the effect of increasing the albedo of snow covered surfaces by diffusing the incoming solar radiation and reducing the infrared radiation reaching the surface. The cloud effect on the albedo of a snow covered surface can be as high as 0.07, as observed by Wang and Zender (2011). Therefore, a variability of cloud cover during the flights can increase the standard deviations in the upper panels of Fig. 4.

The temperature albedo relations in Fig. 4 suggest that the albedo is strongly controlled by the ice thickness and snow cover and that the temperature is a proxy for these parameters. Thicker ice with snow cover, like pack ice, has a lower surface temperature and has, in general, a higher albedo in comparison to very thin, dark nilas ice, which can be found in the polynya region and on just frozen leads. This thin ice, without snow cover, shows relatively warm temperatures near the freezing point and a low albedo. Perovich and Grenfell (1981) showed in laboratory experiments that when young sea ice like nilas becomes thicker, the albedo increases rapidly. The reason is that with the decrease in ice temperature, the amount of brine in the sea ice changes as well, which causes a change in its radiative properties. The temperature acts also as a proxy for the radiative properties of the snow cover and its evolution. Snow metamorphosis is also influenced by the temperature. Colder and younger snow has generally smaller grains sizes than warmer and older snow. An increase in the average radius of the grain increases the length of a photon's travel path through the ice, and decreases the number of opportunities for the photon to scatter out of the snow pack. This increases the probability of the photon being absorbed and reduces the surface albedo (e.g. Gardner and Sharp, 2010).

Due to the fact that the sea ice albedo shows a tendency to increase with decreasing temperature, some numerical models parameterize the albedo with the temperature as the only driving input parameter. Examples of coupled ocean atmosphere models that are participating in the Intergovernmental Panel on Climate Change 4th Assessment Report (IPCC-AR4; Randall et al., 2007) and that use a temperature function to parameterize the albedo are the UK Met Office Hadley Centre Model (UKMO HadCM3; Gordon et al., 2000) and the General Circulation Model (GCM) of the

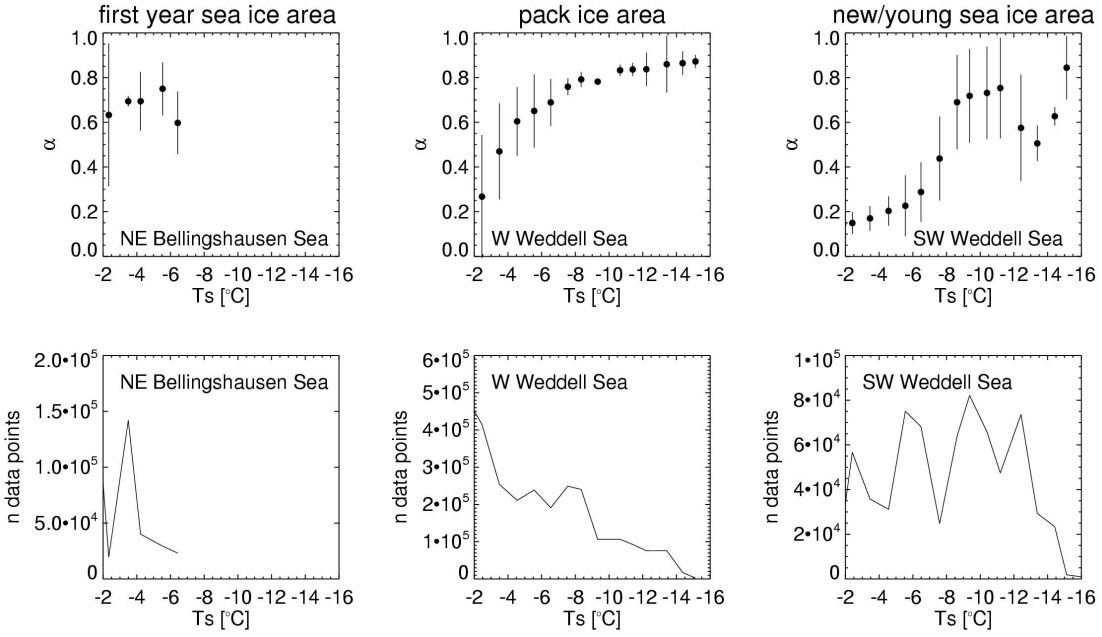

Fig. 4. From left to right, upper row: bin-averaged surface temperature values $\Delta T = 1\,^{\circ}\mathrm{C}$ below freezing point versus albedo of the sea surface measured in the north-eastern Bellingshausen Sea covered mainly with first year ice; the western Weddell Sea pack ice area and the southern part of the western Weddell Sea ice area, covered mainly with new and young ice. Lower row shows number of data points versus surface temperature.

Max-Planck-Institute for Meteorology ECHAM5/MPI-OM of 2005 (Röckner et al., 2003). In this section we do not attempt to investigate the accuracy of the albedo performance of all models participating in the IPCC-AR4. But in the following we rather aim to provide a case study for a comparison of published linear temperature albedo parameterizations with the data we observed in the Weddell and Bellingshausen Seas.

Ross and Walsh (1987) investigated, with a dynamic-thermodynamic sea ice model, the temperature dependence of snow and ice albedo for the Arctic. For their study they modified the Goddard Institute for Space Studies GISS sea ice model of Hansen et al. (1983), by using a temperature dependent albedo parameterization for snow and ice rather than a constant albedo value. The sea surface albedo parameterization of Køltzow (2007) uses also the temperature for the prediction of the albedo, but can also take the influence of melt pond fraction on the sea surface albedo into account. This parameterization was determined from data measured in the Arctic sea ice zone for the Arctic HIRHAM model (Christensen et al., 1996). In the thermodynamic sea ice model described by Ledley (1985), the air temperature, and not the surface temperature, is used to parameterize the sea surface albedo. Ingram et al. (1989) described a linear temperature albedo parameterization for the United Kingdom Met Office general circulation model. The parameterizations used in these models are listed in Table 3. To investigate whether one of these albedo parameterizations describes the sea ice albedo in the Bellingshausen or Weddell Sea realistically, we compared them to our observations.

In Fig. 5 we compare the three examples of albedo parameterization schemes that we listed in Table 3 with our averaged albedo observations for the three sea ice areas as listed in Table 1. In Table 4 statistical measures are given for this comparison. Each albedo parameterization scheme, which is shown in Fig. 5, covers a different surface temperature interval and each scheme shows a different function with decreasing temperature. Comparing the parameterizations with the observations, it is seen that the parameterization of Køltzow (2007) overestimates the sea surface albedo in the north-eastern Bellingshausen Sea, as well as in both Weddell Sea ice areas. The largest normalized mean square error (NMSE) of this parameterization was observed in the Weddell Sea new, young sea ice area, with NMSE = 0.83 with a fractional bias of FB = −0.83, the smallest one in the western Weddell sea with NMSE = 0.01 and FB = −0.10. The parameterization of Køltzow (2007) was developed on the basis of Arctic sea ice. The parameterization of Ross and Walsh (1987) for snow overestimates the sea surface albedo for the north-eastern Bellingshausen Sea (FB = −0.37), as well as of the southern Weddell Sea (FB = −0.78). Here, we observed also the largest NMSE of this albedo parameterization of 0.71. However, the high albedo values in the pack ice area of the western Weddell Sea are captured well by this parameterization, which is reflected in the value of NMSE of close to zero and small FB = −0.03. We cannot

Table 3. Model temperature albedo parameterizations with T_s = surface temperature and T_a = air temperature.

Reference (or origin) of albedo parameterization	Albedo parameterization schemes for sea ice or ice covered sea surface	Temperature range for which the parameterization is valid
United Kingdom Met Office GCM Ingram et al. (1989)	$\alpha = 0.7$ $\alpha = 0.7 - 0.03 \cdot (T_s - 261.2)$ with T_s in K $\alpha = 0.4$	$T_s \leq -11.95\,^\circ$C $-11.95\,^\circ\text{C} < T_s < -1.95\,^\circ$C $T_s = -1.95\,^\circ$C
Dynamic-thermodynamic sea ice model Ross and Walsh (1987) α_s = snow albedo α_i = ice albedo	$\alpha_s = 0.8$ $\alpha_s = 0.65 + 0.03 \cdot (-T_s)$ $\alpha_s = 0.65$ $\alpha_i = 0.65$ $\alpha_i = 0.45 - 0.04 \cdot T_a$ $\alpha_i = 0.45$	$T_s < -5.15\,^\circ$C $-5.15\,^\circ\text{C} < T_s < -0.15\,^\circ$C $T_s = -0.15\,^\circ$C $T_s < -0.15\,^\circ$C $-0.15\,^\circ\text{C} < T_a < 4.85\,^\circ$C T_a =4.85 °C
Køltzow (2007) Version 1, without melt pond	$\alpha_i = 0.84$ $\alpha_i = 0.84 - 0.145 \cdot (2 + T_s)$ $\alpha_i = 0.51$	$T_s \leq -2\,^\circ$C $0\,^\circ\text{C} > T_s > -2\,^\circ$C $T_s \geq 0\,^\circ$C
Thermodynamic sea ice model Ledley (1985)	$\alpha_i = 0.88$ $\alpha_i = 0.88 - 0.00308 \cdot (T_a - 245)$ with T_a in K $\alpha_i = 0.79992 - 0.0322 \cdot (T_a - 271)$ with T_a in K $\alpha_i = 0.51$	$T_a \leq -28.15\,^\circ$C $-28.15\,\text{K} < T_a \leq -2.15\,^\circ$C $-2.15\,^\circ\text{C} < T_a \leq 6.85\,^\circ$C $6.85\,^\circ\text{C} < T_a$

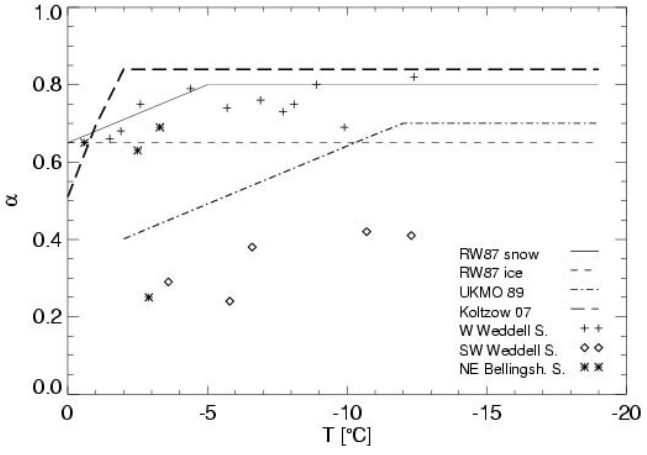

Fig. 5. Examples of albedo parameterization schemes, listed in Table 3, that use the surface temperature as a driving input parameter: *RW87* shows the albedo parameterization scheme of Ross and Walsh (1987) for snow covered and bare ice, respectively; *UKMO 89* is the parameterization of the UK Met Office GC model, as described by Ingram et al. (1989) and *Koltzow 07* a parameterization scheme for the HIRHAM model (Christensen et al., 1996), which is described by Køltzow (2007), Version 1, i.e. with the assumption of no melt pond fraction. The parameterizations are shown only for temperatures below zero degrees. Additionally shown are the averaged albedo data of this study (given in Table 1) for the western Weddell Sea ice area, south-western Weddell Sea ice area and north-eastern Bellingshausen Sea in summer.

verify the second albedo parameterization for ice of Ross and Walsh (1987) with our data, because they required the surface air temperature as an input parameter, which is not available from the aircraft data. The model parameterization, described by Ingram et al. (1989), underestimates the albedo that we observed in the western Weddell Sea (FB = 0.37), with a NMSE = 0.14. This albedo parameterization shows the highest FB = −0.49 for the first year sea ice in the north-eastern Bellingshausen Sea, with a NMSE = 0.25. For the new, young sea ice area, in general, the albedo values are overestimated by this parameterization, with FB = 0.17 and NMSE = 0.03. Summing up, the albedo data observed in the new, young sea ice area are not very well captured by any of the parameterizations tested and are, in general, overestimated. In this area the sea ice was characterized by hardly any snow cover so that sea ice albedo depends mainly on the ice type, its age and/or thickness.

The biggest differences that we see between parameterizations and the measurements are in the areas where thin, young ice prevails. This is probable because most albedo parameterizations were developed on the basis of measurements over thick, consolidated ice. In situ measurements over thin ice are still rare. A further reason for the differences in values between the predicted albedo and the observed albedo in the sea ice areas adjacent to the Antarctic Peninsula could be that most parameterizations are not accounting for such a large variety and mixture of sea ice types. Moreover, the parameterizations are often developed on the basis of Arctic sea ice measurements, so they are probably accounting for Arctic physical sea ice processes, which may not be important in the Antarctic sea ice zone. Most fundamental differences between Arctic and Antarctic sea ice result from

Table 4. Statistical measures compared for three different sea ice areas (as listed in Table 1) and three different parameterizations (as listed in Table 3). The statistical measures are NMSE = the normalized mean square error, COR = correlation coefficient, M Bias = Model bias, and FB = fractional bias ranging from ± 2.

	NMSE	COR	M bias	FB
(A) Comparisons of the statistical measure for three albedo parameterization with averaged albedo values measured in the W Weddell Sea pack ice area.				
Ingram et al. (1989)	0.14	0.79	−0.23	0.37
Ross and Walsh (1987)	0.00	0.78	0.02	−0.03
Køltzow (2007)	0.01	0.60	0.07	−0.10
(B) Same as (A) but for SW Weddell Sea new, young sea ice area.				
Ingram et al. (1989)	0.25	0.80	0.23	−0.49
Ross and Walsh (1987)	0.71	0.41	0.44	−0.78
Køltzow (2007)	0.83	0.41	0.49	−0.83
(C) Same as (A) but for N Bellingshausen Sea first year ice area.				
Ingram et al. (1989)	0.03	0.38	−0.08	0.17
Ross and Walsh (1987)	0.14	0.32	0.22	−0.37
Køltzow (2007)	0.23	0.30	0.30	−0.46

the geographic differences between the two regions, which have an influence on the sea surface albedo. For example, in the Arctic there is only a small fraction of ice advected out of the area and there is less annual variability. In the Antarctic the sea ice can be transported by wind and ocean current northwards, which increases the water fraction of the sea ice areas and enhances the melt processes and decreases the sea surface albedo (Brandt et al., 2005). In the Antarctic frazil crystals in open water make a major contribution to the total ice mass, and the dynamic processes of rafting and ridging are the main mechanisms for the ice growth and thickness changes. The amount of impurities (e.g. black carbon, mineral dust or volcanic ash) on sea ice differs between Arctic and Antarctic, as well as biological processes in the sea ice. In general, impurities lower the albedo of snow covered surfaces, which is described for black carbon by Jacobson (2004). A further example for a physical sea ice process, which differs in the Arctic from the Antarctic, is the melting process of the ice. In the Arctic extensive melt ponds can be observed on sea ice during summer (Hanesiak et al., 2001; Perovich et al., 2002). The inclusion of melt ponds in the albedo scheme is therefore important for the Arctic sea ice areas, because the melt ponds absorb a large portion of solar energy (Pedersen et al., 2009). Although flooded snow and snow-ice can be observed in the Antarctic, melt ponds are not common on Antarctic sea ice. Because they are hardly observed on Antarctic sea ice, we excluded from our comparison a melt pond parameterization. Main conclusions that can be drawn from the comparison of the observations versus the parameterizations are that the comparison indicates that the setting of the minimum-allowed ice albedo should be adjusted to typical Antarctic values (and not to Arctic values). Moreover, discrimination between snow covered and snow free ice in temperature albedo parameterizations should be taken into account.

5 Summary and concluding remarks

The aircraft data of this study show that the sea ice areas adjacent to the Antarctic Peninsula consist of a mixture of different sea ice types with a large range of albedo values. Each compact sea ice area is characterized by a different mixture of certain ice types, but all sea ice areas show values over the entire sea ice albedo that range from 0.07 to more than 0.8 in summer. The north-eastern Bellingshausen Sea ice area is characterized by mainly first year ice, and the western Weddell Sea by mainly multi-year pack ice with leads, with the exception of the south-western part, where a mixture of new, young sea ice prevailed. The observations showed that a characteristic area-averaged sea ice albedo value, which is needed for example as a boundary parameter for a model grid box, should be an average albedo value of different sea ice types, weighted with their frequency distribution. We determined the percentage of the area covered by a certain sea ice albedo range (Fig. 3) and the average albedo of the three areas adjacent to the Antarctic Peninsula (Table 2). We observed the largest mean sea ice albedo value in the western Weddell Sea pack ice area and the smallest mean albedo value in the polynya region, where young, new sea ice prevailed. An intermediate mean albedo value was observed in the north-western Bellingshausen Sea. The high-resolution aircraft measurements indicate a large heterogeneity regarding the surface temperature and albedo in all three sea ice areas. The distribution of the albedo values (Fig. 3) reflects that all main sea ice areas show an alternation of young and old, snow covered and bare sea ice. The regional variation of the mean sea ice albedo is mainly due to the regional variation in the mixture of ice types and its snow cover. Figure 3 shows that all sea ice areas are characterized by spatial heterogeneity of the albedo over the entire albedo range. This albedo heterogeneity strongly affects the radiation budget of the sea ice areas. A specification of the radiative processes is vital for climate and weather forecast models. However, the horizontal resolution of present-day numerical atmospheric models is too coarse to explicitly capture local-scale heterogeneity of the sea ice albedo. The typical resolution of atmospheric GCMs is between 1 and 5 degrees in latitude or longitude (Randall et al., 2007). Mesoscale models have a finer resolution from about 5 to 200 km, and regional-scale models below 5 km. The aircraft measurements show that the subgrid-scale variability of the sea ice albedo can be as small as a few meters. In combination with a spatial heterogeneity of water fraction or snow cover on larger scales, this may result in an area-averaged albedo

that is fundamentally different from the albedo at a particular point. Different methods were developed to describe the subgrid-scale surface albedo heterogeneities in atmospheric models (e.g. Pirazzini and Räisänen, 2008). In this study we determined the averaged albedo for three sea ice areas around the Antarctic Peninsula from the local-scale heterogeneity of the albedo. The averaged albedo value can be approximately assumed to be the effective albedo value for these areas. The area averaged albedo values and the albedo range distribution may be useful for comparison with model predictions or satellite data. Measurements of effective sea ice albedo and temperature are possible, e.g. with optical sensors such as the Moderate Resolution Imaging Spectroradiometer (MODIS). Moreover, the averaged albedo value can be used as an input parameter in numerical models to gives realistic representation of the albedo in the sea ice areas around the Antarctic Peninsula.

Previous studies showed that various factors influence the ice and snow albedo, but the sea surface temperature is often used to parameterize the albedo in climate and weather prediction models. The reason for this is that the temperature is easily available as an input parameter in all models and is a good proxy for various factors influencing the radiative properties of sea ice. We compared the spatially averaged albedo data with published linear temperature albedo parameterizations. In particular, the albedo of areas with new, young ice, which we observed in the southern part of the Weddell Sea, was overpredicted by all the tested parameterizations. An overestimation of the sea surface albedo implicates a too low energy input into the ice covered ocean system. One reason that the data are not fitted well by all parameterizations might be that the temperature can act as a proxy for different factors that influence the radiative properties of sea ice. On the one hand, the temperature can act as proxy mainly for the ice thickness and on the other hand, mainly for the conditions of the snow cover on sea ice. For thin, bare, new and young sea ice, which we observed in particular in the polynya region and on just-frozen leads, the sea ice albedo is mainly influenced by the sea ice thickness. We observed a rapid increase of the albedo with increase in sea ice thickness, i.e. decrease in temperature, but the albedo values are lower than those of sea ice that have the same temperature, but are snow covered. On the other hand, the data showed that the albedo of snow covered sea ice was generally much larger than that of snow free ice and increases more slowly with decreasing temperature. This indicates that for snow covered sea ice the temperature acts, in particular, as a proxy for the snow conditions and snow metamorphosis and the sea ice thickness becomes less important. Commonly used parameterizations use the surface temperature as a proxy for the snow cover and metamorphosis on the ice and not as proxy for the ice thickness, which is most important for thin, new sea ice. Summing up, the study shows that one linear temperature albedo parameterization can be only a rough approximation for sea ice areas, that show a mixture of bare and snow covered sea ice. We observed such a mixture of bare and snow covered sea ice in all three sea ice areas adjacent to the Antarctic Peninsula, but with various frequency distributions of ice types. The comparison of our data with model parameterization, which is shown in Fig. 5, can help to interpret GCM albedo simulation for Antarctic sea ice areas that show a mixture of new, young sea ice, first year ice and multi-year pack ice.

The large number of factors that influence the radiative properties of sea ice implies that for a more accurate albedo parameterization, further input parameters should be taken into account and have to be available as input parameters within the model. There is, in particular, a need for a better parameterization of the albedo over thin/new sea ice. Such a parameterization will be particularly important as model resolution increases and as models are able to resolve features such as large polynyas, where thin ice prevails. More sophisticated model parameterizations do already exist in more complex models. They use as an input parameter not only the temperature, but also the ice thickness (e.g. Manabe et al., 1992; Flato and Brown, 1996), and snow cover of ice, e.g. in the Arctic regional climate system model (ARCSYM) described by Lynch et al. (1995). Another example is the Los Alamos sea ice model (CICE), as used in the Community Climate System Model (CCSM3). CICE predicts the albedo with a complex parameterization, including temperature, spectral bands, thickness of sea ice and snow cover (Hunke and Lipscomb, 2008). Lui et al. (2007) tested such complex albedo parameterizations for an Arctic sea ice area. They tested albedo parameterizations that depended not only on surface temperature, but also on surface type (snow or ice), snow depth, ice thickness and spectral band by comparing them to in situ measurements made during the Surface Heat Budget of the Arctic Ocean (SHEBA) project. Their study showed that the simulated surface albedos differed substantially, depending on the complexity of the parameterization used. They showed that, by using a more complex albedo parameterization, a more realistic ice distribution can be predicted for the Arctic sea ice area. However, for a determination or validation of such complex albedo parameterizations for the sea ice areas adjacent to the Antarctic Peninsula further area-covering observations of additional surface parameters, like averaged sea ice thickness and snow conditions have to be conducted.

Acknowledgements. This study is a contribution to the British Antarctic Survey's program "Polar Science for Planet Earth". We thank the BAS Air Unit and staff at Rothera Research Station for their assistance with the measurement campaigns. We thank P. Fretwell for providing the map in Fig. 1.

Edited by: M. Van den Broeke

References

Allison, I., Brandt, R. E., and Warren, S. G.: East Antarctic sea ice: albedo, thickness distribution, and snow cover, J. Geophys. Res., 98, 12417–12429, 1993.

Bannehr, L. and Glover, V.: Preprocessing of airborne Pyranometer data, NCAR Technical Note, 364, 1–35, 1991.

Bracegirdle, T. J., Connolley, W. M., and Turner, J.: Antarctic climate change over the twenty first century, J. Geophys. Res., 113, D03103, doi:10.1029/2007JD008933, 2008.

Brandt, R. E., Warren, S. G., Worby, A. P., and Grenfell, T. C.: Surface Albedo of the Antarctic sea ice zone, J. Climate, 18, 3606–3622, 2005.

Burns, S. P., Khelif, D., Friehe, C. A., Hignett, P., Williams, A. G., Grant, A. L. M., Hacker, J. M., Hagan, D. E., Serra, Y. L., Rodgers, D. P., Bradley, E. F., Weller, R. A., Fairall, C. W., Anderson, S. P., Paulson, C. A., and Coppin, P. A.: Comparison of aircraft, ship, and buoy radiation and SST measurements from TOGA COARE, J. Geophys. Res., 105, 15627–15652, 2000.

Cavalieri, D. J. and Parkinson, C. L.: Antarctic sea ice variability and trends, 1979–2006, J. Geophys. Res., 113, C07004, doi:10.1029/2007JC004564, 2008.

Christensen, J. H., Christensen, O. B., Lopez, P., van Meijgaard, E., and Botzet, M.: The HIRHAM4 Regional Atmospheric Climate Model, Scientific Report, Danish Meteorological Institute, Copenhagen, 1996.

Curry, J. A., Schramm, J., Perovich, D. K., and Pinto, J. O.: Applications of SHEBA/FIRE data to evaluation of snow/ice albedo parameterizations, J. Geophys. Res., 106, 15345–15355, 2001.

Flato, G. M. and Brown, R. D.: Variability and climate sensitivity of landfast Arctic sea ice, J. Geophys. Res., 101, 25767–25777, 1996.

Gardner, A. S. and Sharp, M. J.: A review of snow and ice albedo and the development of a new physically based broadband albedo parameterization, J. Geophys. Res., 115, F01009, doi:10.1029/2009JF001444, 2010.

Gordon, C., Cooper, C., Senior C. A., Banks, H., Gregory, J. M., Johns, T. C., Mitchell, J. F. B., and Wood, R.: The simulation of SST, sea ice extents and ocean heat transports in a version of the Hadley Centre coupled model without flux adjustments, Clim. Dynam., 16, 147–168, 2000.

Grenfell, T. C. and Perovich, D. K.: Spectral albedos of sea ice and incident solar irradiance in the southern Beaufort Sea, J. Geophys. Res., 89, 3573–3580, 1984.

Grenfell, T. C., Warren, S. G., and Mullen, P. C.: Reflection of solar radiation by the Antarctic snow surface at ultraviolet, visible and near-infrared wavelengths, J. Geophys. Res., 99, 18669–18684, 1994.

Hanesiak, J. M., Barber, D. G., De Abreu, R. A., and Yackel, J. J.: Local and regional albedo observations of arctic first-year sea ice during melt ponding, J. Geophys. Res., 106, 1005–1016, doi:10.1029/1999JC000068, 2001.

Hansen, J., Russell, G., Rind, D., Stone, P., Lacis, A., Lebedeff, S., Ruedy, R., and Travis, L.: Efficient three-dimensional global models for climate studies: models I and II, Mon. Weather Rev., 111, 609–662, 1983.

Hibler III, W. D. and Bryan, K.: A diagnostic ice-ocean model, J. Phys. Oceanogr., 17, 987–1015, 1987.

Hunke, E. C. and Lipscomb, W. H.: CICE: The Los Alamos Sea Ice Model, Documentation and Software User's Manual, Version 4.0, T-3 Fluid Dynamics Group, Los Alamos National Laboratory, Tech. Rep. LA-CC-06-012, 2008.

Ingram, W. J., Wilson, C. A., and Mitchell, J. F. B.: Modeling climate change: An assessment of sea ice and surface albedo feedbacks, J. Geophys. Res., 94, 8609–8622, 1989.

Jacobson, M. Z.: Climate response of fossil fuel and biofuel soot, accounting for soot's feedback to snow and sea ice albedo and emissivity, J. Geophys. Res., 109, D21201, doi:10.1029/2004JD004945, 2004.

Jenkins, A. and Jacobs, S.: Circulation and melting beneath George VI Ice Self, Antarctica, J. Geophys. Res., 113, C04013, doi:10.1029/2007JC004449, 2008.

King, J. C., Lachlan-Cope, T. A., Ladkin R. S., and Weiss A.: Airborne measurements in a stable boundary layer over the Larsen Ice Shelf, Antarctica, Bound.-Lay. Meteorol., 127, 413–428, 2008.

Køltzow, M.: The effect of a new snow and sea ice albedo scheme on regional climate model simulations, J. Geophys. Res., 112, DO7110, doi:10.1029/2006JD007693, 2007.

Ledley, T.: Sensitivity of a thermodynamic sea ice model with leads to time step size, J. Geophys. Res., 90, 2251–2260, 1985.

Liu, J., Curry, J. A., and Martinson, D. G.: Interpretation of recent Antarctic sea ice variability, Geophys. Res. Lett., 31, L02205, doi:10.1029/2003GL018732, 2004.

Liu, J., Zhang, Z., Inoue, J., and Horton, R. M: Evaluation of snow/ice albedo parameterizations and their impacts on sea ice simulations, Int. J. Climatol., 27, 81–91, 2007.

Lynch, A. H., Chapman, W. L., Walsh, J. E., and Weller, G.: Development of a regional climate model of the Western Arctic, J. Climate, 8, 1555–1570, 1995.

Manabe, S., Spelman, M. J., and Stouffer, R. J.: Transient responses of a coupled ocean-atmosphere model to gradual changes of atmospheric CO_2. Part II: Seasonal response, J. Climate, 5, 105–126, 1992.

Mellor, G. L. and Kantha, L.: An ice-ocean coupled model, J. Geophys. Res., 94, 10937–10954, 1989.

Nicholls, K. W., Østerhus, S., Makinson, K., and Johnson, M. R.: Oceanographic conditions south of Berkner Island, beneath Filchner-Ronne Ice Shelf, Antarctica, J. Geophys. Res., 106, 11481–11492, 2001.

Nicholls, K. W., Boeme, S. L., Biuw, M., and Fedak, M. A.: Wintertime ocean conditions over the Southern Weddell Sea continental shelf north of Ronne Ice Shelf, Antarctica, Geophys. Res. Lett., 35, L21605, doi:10.1029/2008GL035742, 2008.

Parkinson, C. L. and Washington, W. M.: A large-scale numerical model of sea ice, J. Geophys. Res., 84, 311–337, 1979.

Pedersen, C. A., Röckner, E., Lüthje, M., and Winther, J.-G.: A new sea ice albedo scheme including melt ponds for ECHAM5 general circulation model, J. Geophys. Res., 114, DO8101, doi:10.1029/2008JD010440, 2009.

Perovich, D. K. and Grenfell, T. C.: Laboratory studies of the optical properties of young sea ice, J. Glaciol., 27, 331–346, 1981.

Perovich, D. K., Tucker III, W. B., and Ligett, K. A.: Aerial observation of the evolution of ice surface conditions during summer, J. Geophys. Res., 107, 8048, doi:10.1029/2000JC000449, 2002.

Pirazzini, R.: Surface albedo measurements over Antarctic sites in summer, J. Geophys. Res., 109, D20118, doi:10.1029/2004JD004617, 2007.

Pirazzini, R. and Räisänen , P.: A method to account for surface albedo heterogeneity in single-column radiative transfer calculations under overcast conditions, J. Geophys. Res., 113, D20108, doi:10.1029/2008JD009815, 2008.

Predoehl, M. C. and Spano, A. F.: Airborne albedo measurements over the Ross Sea, October–November 1962, Mon. Weather Rev., 93, 687–696, 1965.

Randall, D. A., Wood, R. A., Bony, S., Colman, R., Fichefet, T., Fyfe, J., Kattsov, V., Pitman, A., Shukla, J., Srinivasan, J., Stouffer, R. J., Sumi, A., and Taylor, K. E.: Climate Models and Their Evaluation, in: Climate Change 2007: The Physical Science Basis. Contribution of Working Group I to the Fourth Assessment Report of the Intergovernmental Panel on Climate Change, edited by: Solomon, S., Qin, D., Manning, M., Chen, Z., Marquis, M., Averyt, K. B., Tignor, M., and Miller, H. L., Cambridge University Press, Cambridge, United Kingdom and New York, NY, USA, 2007.

Renfrew, I. A., King, J. C., and Markus, T.: Coastal polynyas in the southern Weddell Sea: variability of the surface energy budget, J. Geophys. Res., 107, 3063, doi:10.1029/2000JC000720, 2002.

Röckner, E., Bäumel, G., Bonaventura, L., Brotkopf, R., Esch, M., Giorgetta, M., Hagemann, S., Irchner, I., Kornblüh, L., Manzini, E., Rhodin, A., Schlese, U., Schulzweida, U., and Tomkins, A.: The atmospheric general circulation model ECHAM5-Part1 Tech. Rep. 349, Max-Planck-Institute for Meteorology, Hamburg, 2003.

Ross, B. and Walsh, J. E.: A comparison of simulated and observed fluctuations in summertime Arctic surface albedo, J. Geophys. Res., 92, 13115–13125, 1987.

Schnack-Schiel, S.: Die Winter-Expedition mit FS Polarstern in die Antarktis (ANT V/1-3) (The Winter-Expedition of RV Polarstern to the Antarctic (ANT V/1-3)), Berichte zur Polarforschung, 39, Alfred-Wegener Institut für Polarforschung, 259 pp., 1987.

Turner, J., Lachlan-Cope, T. A., Colwell, S. T., and Marshall, G. J.: Significant warming of the Antarctic winter troposphere, Science, 311, 1914–1917, 2006.

Vashisth, P.: Effect of clouds and free water on snow albedo, Bull. Glaciol. Res., 22, 63–67, 2005.

Vihma, T., Johansson, M. M., and Launiainen, J.: Radiative and turbulent surface heat fluxes over sea ice in the western Weddell Sea in early summer, J. Geophys. Res., 114, C04019, doi:10.1029/2008JC004995, 2009.

Wang, X. and Zender, C. S.: Arctic and Antarctic diurnal and seasonal variations of snow albedo from multiyear Baseline Surface Radiation Network measurements, J. Geophys. Res., 116, F03008, doi:10.1029/2010JF001864, 2011.

Weiss, A. I., King, J. C., Lachlan-Cope, T. A., and Ladkin, R.: On the effective aerodynamic and scalar roughness length of Weddell Sea ice, J. Geophys. Res., 116, D19119, doi:10.1029/2011JD015949, 2011.

Wiscombe, W. J., and Warren, S. G.: A model of the spectral albedo of snow, I: pure snow, J. Atmos. Sci., 37, 2712–2733, 1980.

Zhou, X., Li, S., Morris, K., and Jeffries, M. O.: Albedo of summer snow on sea ice, Ross Sea, Antarctica, J. Geophys. Res., 112, D16105, doi:10.1029/2006JD007907, 2007.

Zwally, H. J., Comiso, J. C., Parkinson, C. L., Cavalieri, D. J., and Gloersen, P.: Variability of Antarctic sea ice 1979–1998, J. Geophys. Res., 107, 3041, doi:10.1029/2000JC000733, 2002.